New approaches to the synthesis of acicular α-FeOOH and cobalt-modified iron oxide particles

P. C. Kuo and T. S. Tsai
The Graduate Institute of Materials Engineering, National Taiwan University, Taipei, Taiwan, Republic of China

(Received 31 October 1988; accepted for publication 24 January 1989)

Formation of acicular α-FeOOH particles from the reaction system of $FeCl_2$-NaOH is studied. It is found that acicular α-FeOOH particles with a particle size of about 0.5 μm and axial ratio of about 10 can be obtained by oxidizing the mixed solution of $FeCl_2$ and NaOH with a molar ratio of $NaOH/FeCl_2$ larger than 2. New acicular Co-γ-Fe_2O_3 particles are synthesized by absorbing Co^{2+} ions on the surface of acicular α-FeOOH particles followed by dehydrating, reduction, and oxidation. We find that using N_2 as dehydrating atmosphere is better than air or H_2. After reduction, variations of the coercivity of Co-Fe_3O_4 particles with various cooling rates are investigated. The transformation temperature of Co-$Fe_3O_4 \rightarrow$ Co-γ-Fe_2O_3 is about 300 °C for the particles with cobalt content $(Co/Co + Fe) < 12$ mol %. Distributions of Co^{2+} and Fe^{2+} ions in the particles are measured by the dissolution method. Coercivity of the acicular Co-γ-Fe_2O_3 particles between 400 and 1200 Oe can be controlled by the cobalt content and additional anneal in N_2.

I. INTRODUCTION

Acicular γ-Fe_2O_3 particles have long been used as recording materials. However, for the requirement of high-density recording, pure γ-Fe_2O_3 particles seem to reach their limit due to low coercivity ($H_c < 500$ Oe). Bickford and co-workers[1,2] have found that adding a small amount of cobalt in the iron oxide particles will largely increase the magnetocrystalline anisotropy of the oxide. Thus, the coercivity of particles can be increased pronouncedly. But, owing to the thermal instability of the magnetic properties of cobalt ferrite, acicular cobalt-modified iron oxide particles with a coercivity higher than 500 Oe were invented lately to overcome this shortcoming.[3,4] Since the cobalt ferrite only formed on the surface layer of the acicular particles, thermal instability of the particle coercivity is reduced. Now, acicular cobalt-modified iron oxide particles are widely used in commercial home video tapes and compact cassette tapes.

At present, acicular cobalt-modified iron oxide particles are usually synthesized by the following two methods: (1) Co-epitaxial method: These kinds of particles are synthesized by heating the γ-Fe_2O_3 particles in alkaline solution containing cobaltous and ferrous ions so as to crystallize $CoFe_2O_4$ on the surface of γ-Fe_2O_3 particles.[5-7] (2) Co-substituted method: These kinds of particles are synthesized by heating the γ-Fe_2O_3 particles in the solution of cobaltaous sulfate and sodium citrate using an autoclave.[8] During hydrothermal treatment, γ-Fe_2O_3 is reduced to the oxide phase near Fe_3O_4, and cobalt ions are substituted into the Fe_3O_4 lattices.

In this paper, a new method for the synthesis of acicular cobalt-modified iron oxide particles from α-FeOOH particles is presented. The formation conditions of acicular α-FeOOH particles in an $FeCl_2$-NaOH reaction system are also investigated. (Usually, acicular α-FeOOH particles are synthesized from the reaction system of $FeSO_4$-NaOH.[9])

This paper includes the following three parts: (1) constructing the phase diagram of $FeCl_2$-NaOH reaction system, (2) preparing the acicular α-FeOOH particles and cobalt-absorbed α-FeOOH particles (Co-α-FeOOH particles), and (3) investigating the effect of heat treatment on the magnetic properties of Co-Fe_3O_4 and Co-γ-Fe_2O_3 particles. In addition, the concentration profile of cobalt in the particles determined by the "dissolution method" is studied, and the relationships between the cobalt concentration profile and magnetic properties of the particles are also investigated.

II. EXPERIMENT

Acicular α-FeOOH particles are prepared by the coprecipitation method. The starting materials are $FeCl_2$ and NaOH. A $FeCl_2$ solution is prepared by adding $FeCl_2 \cdot 4H_2O$ into de-ionized water and stirring to complete dissolution. The NaOH solution is prepared by dissolving NaOH into de-ionized water. These two solutions are prepared with various concentrations. The prepared $FeCl_2$ and NaOH solutions are mixed together by stirring. The amounts of the $FeCl_2$ and NaOH solutions are the same before mixing. Air is bubbled uniformly into the mixed solution to promote an oxidizing reaction.

Acicular α-FeOOH particles which precipitated from the mixed solution with $NaOH/FeCl_2$ molar ratio > 2 are coated with cobalt. It is made by dripping the $CoSO_4$ solution slowly into the mixed solution for which α-FeOOH particles have been precipitated. After coating, the Co-α-FeOOH particles are washed and filtered, then dried at 60 °C. The heat treatment for producing Co-γ-Fe_2O_3 particles from Co-α-FeOOH includes three stages:

$$\text{Co-}\alpha\text{-FeOOH} \xrightarrow[T \sim 300\,^{\circ}\text{C}]{\text{dehydration}} \text{Co-}\alpha\text{-}Fe_2O_3, \quad (1)$$

 0021-8979/89/114349-08$02.40

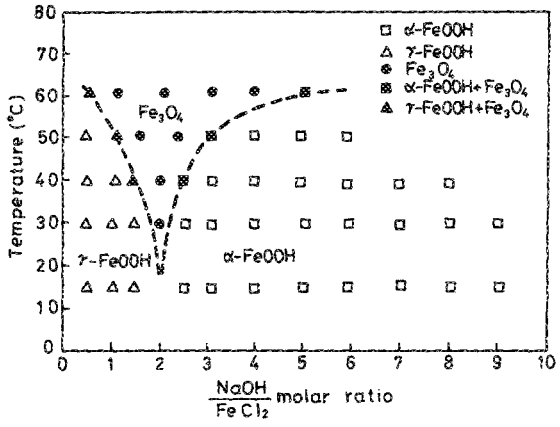

FIG. 1. Effects of $NaOH/FeCl_2$ molar ratio and reaction temperature on the formation of various kinds of precipitates for the $FeCl_2$-NaOH reaction system.

$$\text{Co-}\alpha\text{-}Fe_2O_3 \xrightarrow[T=350\,^\circ\text{C}]{\text{reduction in } H_2} \text{Co-}Fe_3O_4, \tag{2}$$

$$\text{Co-}Fe_3O_4 \xrightarrow[T=300\,^\circ\text{C}]{\text{oxidation in air}} \text{Co-}\gamma\text{-}Fe_2O_3. \tag{3}$$

The crystal structure of the particles is investigated by x-ray diffraction using Fe-filtered Co$K\alpha$ radiation. The particle shape, size, and morphology are observed by a transmission electron microscope. Magnetic properties of the particles are measured with a vibrating sample magnetometer. The Fe^{2+}- and Fe^{3+}-ion content in particles is measured by means of chemical analysis. The value of the Co/Co + Fe molar ratio of the particles is determined by atomic absorption analysis. The concentration profiles of cobalt and iron in the particle are determined by the "dissolution method." In this method, the particles are dissolved in HCl. During dissolving, a small amount of the solution is taken out every few minutes. These sampled solutions are analyzed by atomic absorption analysis. The dissolution rate of the particles can be controlled by adjusting the concentration of HCl.

III. RESULTS AND DISCUSSION

The formation of the precipitates of the $FeCl_2$-NaOH reaction system is affected by many factors. Figure 1 shows the effects of reaction temperature and $NaOH/FeCl_2$ molar ratio of the solution on the formation of various kinds of the final precipitates. The dotted lines which are used to separate different kinds of the precipitates in Fig. 1 cannot be exactly localized, because some other factors such as oxidizing rate and concentration of the solution may affect the result.

According to our experiment, reaction temperature may affect the particle size, phase, and the reaction time. The precipitate at high reaction temperature is Fe_3O_4, as shown in Fig. 1. Its shape is granular and the color is black. At lower reaction temperature and lower $NaOH/FeCl_2$ molar ratio, the final precipitate is γ-FeOOH. Its shape is lath and veinlike, and its color is orange. At lower reaction temperature and higher $NaOH/FeCl_2$ molar ratio, the final precipitate is α-FeOOH. Its shape is long and rodlike, and the color is yellow. Figures 2(a), 2(b), and 2(c) show the particles of γ-FeOOH, α-FeOOH, and Fe_3O_4 + γ-FeOOH + α-FeOOH, respectively. In each phase region of Fig. 1, the reaction rate and the particle size are increased when the reaction temperature is raised, except for Fe_3O_4 particles. Figures 3(a) and 3(b) show the α-FeOOH particles which precipitated at the reaction temperature of 15 and 30 °C respectively. It is evident that the particle size of Fig. 3(b) is larger than that of Fig. 3(a). The length of the α-FeOOH particles of Fig. 3(b) is about 0.5 μm, and the axial ratio is about 10. In general, at the same reaction temperature, the higher $NaOH/FeCl_2$ molar ratio of the solution will result in larger α-FeOOH particle size.

The concentration of the solution will also affect the particle shape and size of the precipitates. Figure 4 shows two kinds of precipitated γ-FeOOH particles. Their solutions have the same $NaOH/FeCl_2$ molar ratio, but with different concentrations. Concentrations of the solutions of Figs. 4(a) and 4(b) are 0.10 M and 0.35 M, respectively. For γ-FeOOH particles, the higher concentration of the solution will result in larger and longer particles. For α-FeOOH particles, the higher concentration can also get larger particles, but the axial ratio (length/width) of the particles is less than that with lower concentration.

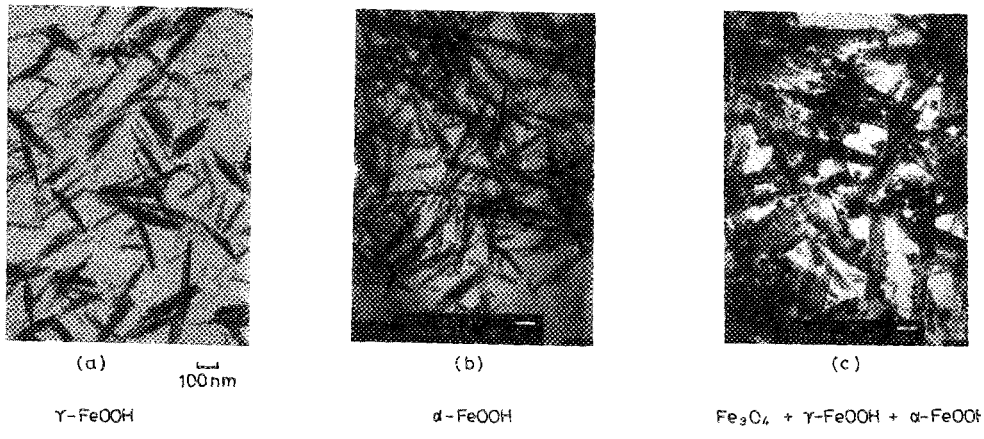

FIG. 2. Electron micrographs of various kinds of precipitated particles: (a) γ-FeOOH, (b) α-FeOOH, and (c) Fe_3O_4 + γ-FeOOH + α-FeOOH.

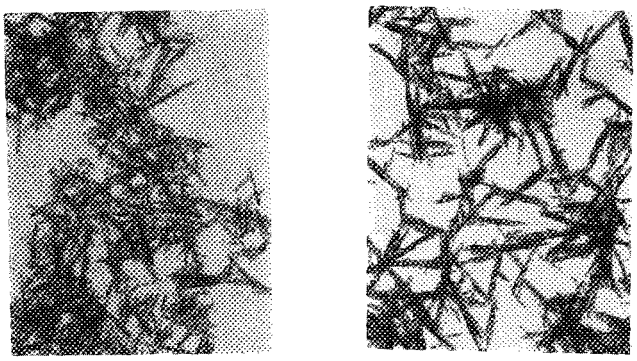

FIG. 3. Electron micrographs of α-FeOOH particles which percipitated at the reaction temperatures of (a) 15 °C and (b) 30 °C.

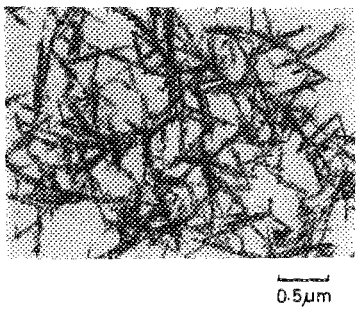

FIG. 5. Electron micrograph of the α-FeOOH particles for which the cobalt coating failed.

Acicular Co-α-FeOOH particles are prepared by absorbing cobalt on the surface of α-FeOOH particles which are shown in Fig. 3(b). In the coating process, the dripping of $CoSO_4$ solution into the α-FeOOH slurry must be very slow. Fast dripping may precipitate new small $Co(OH)_2$ particles with granular shape, as shown in Fig. 5.

After dehydrating from Co-α-FeOOH in different atmospheres, morphologies of the particles with cobalt content of (Co/Co + Fe) = 6 mol % are shown in Fig. 6. Although the dehydration temperature and dehydration time are the same, their morphologies are different. There is only a small amount of little pores within the particle dehydrated in N_2, as shown in Fig. 6(a). The size and number of pores within the particles are increased when the Co-α-FeOOH particles are dehydrated in air, as shown in Fig. 6(b). If the particles are dehydrated in H_2, they will have many big pores within the particles, as shown in Fig. 6(c). These pores come from the loss of H_2O in Co-α-FeOOH particles during dehydrating. Since the particles which were dehydrated in N_2 have a more smooth surface and less pores than those dehydrated in air or H_2, N_2 is a better dehydration atmosphere. It is still not understood why the size and number of pores within the particles which were dehydrated in different atmospheres are different.

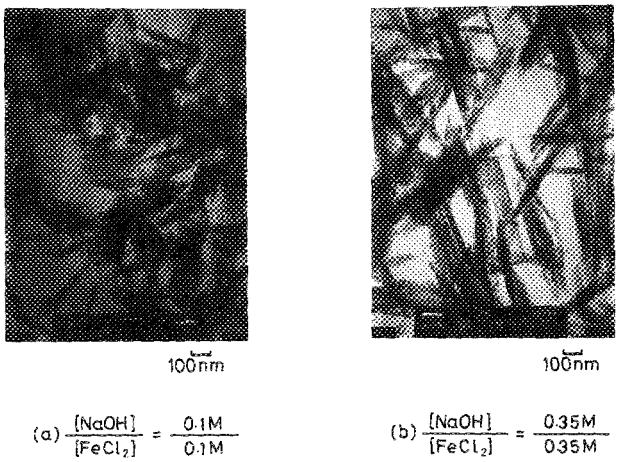

FIG. 4. Electron micrographs of the γ-FeOOH particles which precipitated at different concentrations of the solutions.

For the reduction of Co-α-Fe_2O_3 particles to Co-Fe_3O_4 particles, Fig. 7 shows the variation of saturation magnetization σ_s with reduction time of the particles in which cobalt content (Co/Co + Fe) is 6 mol %. In order to avoid the effects of other factors, the Co-α-Fe_2O_3 particles which were used in the reduction stage were dehydrated from Co-α-FeOOH in air.

The σ_s of the particles is increased with reduction time to about 78 emu/g, then decreased, and reaches a minimum value at about 20 min, then increased rapidly. From the observations of x-ray diffraction patterns, we find that when the reduction time is longer than 10 min, the nonmagnetic phase FeO has appeared. The content of FeO is increased with reduction time and reaches a maximum value at about 20 min. This overreduction phenomenon is increased continuously with reduction time. When the reduction time is longer than 20 min, another phase, α-Fe, appears. The amount of α-Fe phase is increased with reduction time, and so the σ_s of the particles increases rapidly with reduction time when the reduction time is longer than 20 min. Variation of the particles' coercivity H_c with reduction time is similar to that of σ_s, as shown in Fig. 8. But the minimum value of H_c occurs at about 15 min of reduction time which is different to that of σ_s. This may be due to the sintering of particles. Figure 9(a) shows the particles after 10 min reduction, and Fig. 9(b) is the particles after 15 min reduction. Some particles of Fig. 9(b) are sintered together, and the shape anisotropy of the particles is lower than that of Fig. 9(a). Thus, the decrease of H_c with reduction time is due to both the decreasing of particle-shape anisotropy and the containing of the FeO phase. As the reduction time is longer than 20 min, the increasing of H_c may be due to the increase of α-Fe content and the diffusion of Co^{2+} ions into the particles.

For the oxidation of Co-Fe_3O_4 to Co-γ-Fe_2O_3, the suitable oxidation temperature is obtained by means of thermogravimetric analysis (TGA). The Co-Fe_3O_4 particles are heated in air with a heating rate of 10 °C/min. Figure 10 shows a representative case of the variation of particle weight with temperature. Below 150 °C, the weight of the particles is decreased with increasing temperature. This is

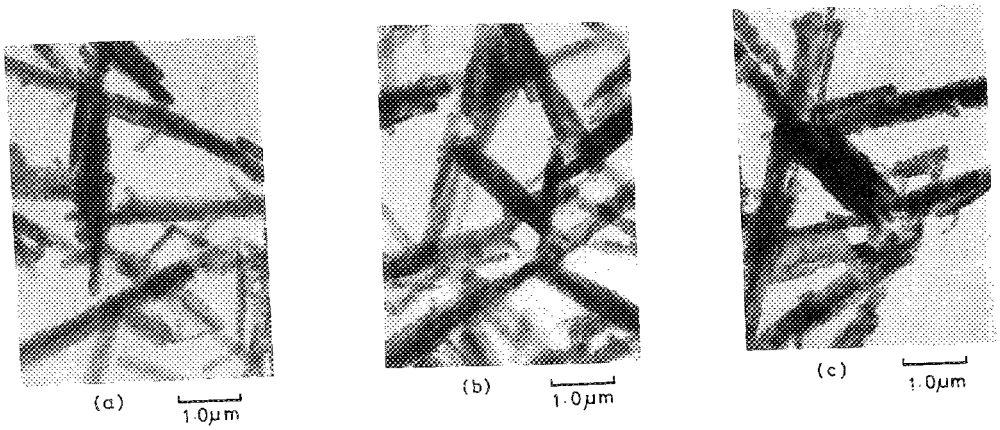

FIG. 6. Electron micrographs of the particles which dehydrated from Co-α-FeOOH particles in various atmospheres: (a) N_2, (b) air, and (c) H_2.

attributed to the loss of water which is absorbed on the surfaces of the particles. As the temperature goes above 150 °C, the weight of the particles is increased with increasing temperature. This is due to the gradual transformation of Co-$Fe_3O_4 \rightarrow (\text{Co-}Fe_3O_4)_{1-x}(\text{Co-}\gamma\text{-}Fe_2O_3)_x \rightarrow \text{Co-}\gamma\text{-}Fe_2O_3$. Since the weight of the particles is not increased again when the temperature is higher than 300 °C, the transformation is complete at about 300 °C. For the particles with $(\text{Co/Co} + \text{Fe}) < 12$ mol %, their transformation temperatures are about the same.

During oxidation, Fig. 11 shows the variation of σ_s with Fe^{2+}-ion content of the particles in which cobalt content $(\text{Co/Co} + \text{Fe})$ is 6 mol %. The σ_s of the particles is decreased as the oxidation degree x increased. This may be explained by the fact that the σ_s of Co-Fe_3O_4 (Fe^{2+}/total Fe = 33%) is larger than that of Co-γ-Fe_2O_3 (Fe^{2+}/total Fe = 0%). It has been reported that a partially oxidized Fe_3O_4 particle is a mixture of two phases, Fe_3O_4 and γ-Fe_2O_3.[10] In order to identify whether our partially oxidized Co-Fe_3O_4 particle is a homogeneous solid solution or a mixture of two phases, Fe_3O_4 and γ-Fe_2O_3, the particles were analyzed by the dissolution method. Figure 12 shows the Fe^{2+} content versus dissolved ratio of the particles in which total Fe^{2+} content (Fe^{2+}/total Fe) is 15 mol %. The dissolved amount of the particles is increased as the dissolved ratio increases. The dissolved ratio of 1.0 indicates that the particles are completely dissolved. From Fig. 12 we can see that at inner part of the particle, the amount of Fe^{2+} ions is much more than that at outer part of the particle. This reveals that the inner part of the particle is Fe_3O_4 phase and the particle is a mixture of two phases.

Figure 13 shows the relationships between the coercivity and cobalt content of the Co-γ-Fe_2O_3 particles. Coercivity of the particles is increased as cobalt content is increased, as shown in curve A. Coercivity of the pure γ-Fe_2O_3 particles is 315 Oe only. But the coercivity of $(\text{Co/Co} + \text{Fe}) = 10$ mol % Co-γ-Fe_2O_3 particles will be higher than 700 Oe. If these particles are annealed in N_2 at 350 °C for 3 h, their coercivities are shown in curve B. Comparing curve B with curve A we can see that the increment of the coercivity is approximately proportional to the cobalt content of the particles. The coercivity of pure γ-Fe_2O_3 particles is unchanged after annealing. But the coercivity of Co-γ-Fe_2O_3 particles with $(\text{Co/Co} + \text{Fe}) = 10$ mol % will be raised from 720 to 1120 Oe. By using the "dissolution method" to measure the distribution of Co^{2+} ions in the particles, we confirm that the increasing of the coercivity of Co-γ-Fe_2O_3 particles after annealing is mainly due to the diffusion of Co^{2+} ions into the particles.

The coercivity of Co-Fe_3O_4 particles is larger than that of Co-γ-Fe_2O_3, if they have the same cobalt content. However, the coercivity of Co-Fe_3O_4 particles is unstable even at room temperature. Curve A of Fig. 14 shows the dependence of H_c on the Fe^{2+} ions content of $(\text{Co-}Fe_3O_4)_{1-x}(\text{Co-}\gamma\text{-}Fe_2O_3)_x$ particles in which cobalt content $(\text{Co/Co} + \text{Fe})$ is

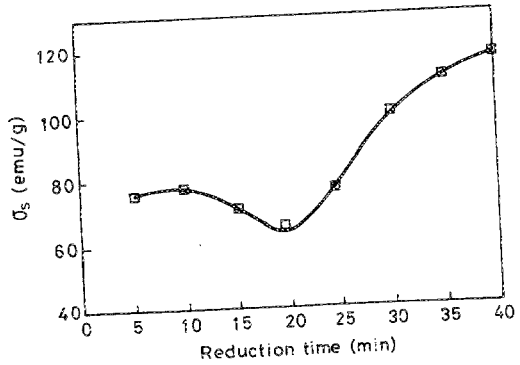

FIG. 7. Relationship between the particles' saturation magnetization and reduction time.

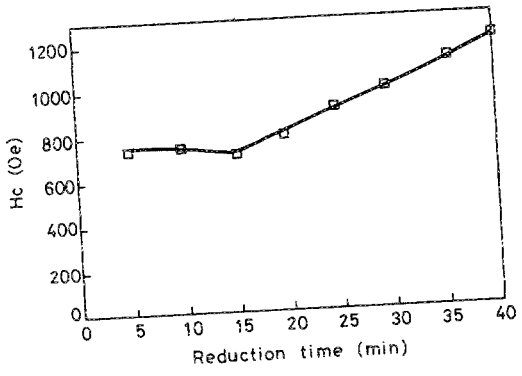

FIG. 8. Variation of the particles' coercivity with reduction time.

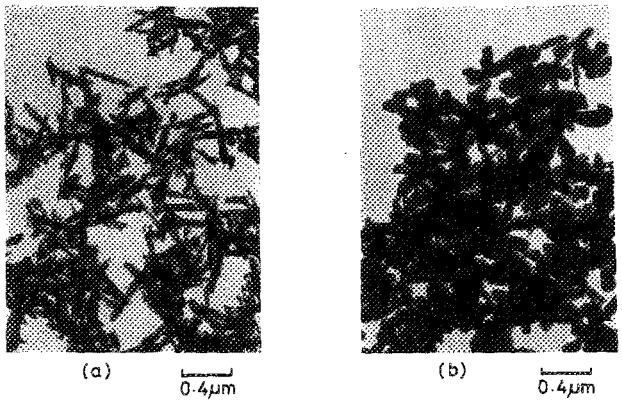

FIG. 9. Electron micrographs of the particles which are reduced from Co-α-Fe_2O_3 with the reduction time of (a) 10 min and (b) 15 min.

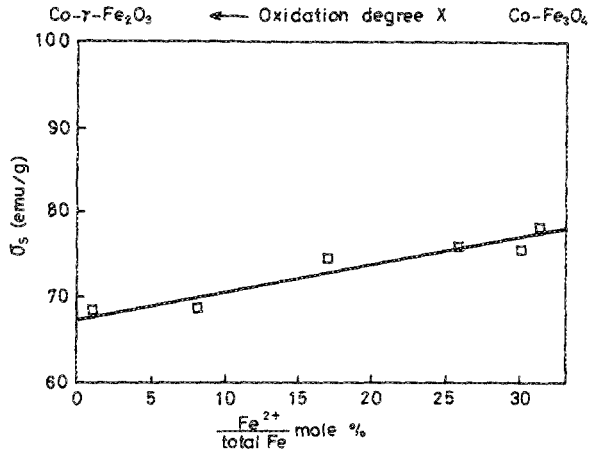

FIG. 11. Variation of σ_s with the degree of oxidation in the transformation of $Co\text{-}Fe_3O_4 \rightarrow (Co\text{-}Fe_3O_4)_{1-x}(Co\text{-}\gamma\text{-}Fe_2O_3)_x \rightarrow Co\text{-}\gamma\text{-}Fe_2O_3$. Cobalt content (Co/Co + Fe) of the particles is 6 mol %.

6 mol %. Maximum value of H_c occurs at about 20 mol % content of Fe^{2+} ions. If these particles are aged at room temperature for 80 days, their coercivity will change from curve A to curve B. The coercivity difference of curve A and curve B is increased when the content of Fe^{2+} ions is increased. This indicates that at room temperature, the stability of the coercivity of $(Co\text{-}Fe_3O_4)_{1-x}(Co\text{-}\gamma\text{-}Fe_2O_3)_x$ particles is increased as the oxidation degree x of the particles is increased. This phenomenon may be due to the migration of Co^{2+} ions in the oxide lattices. Yanase[11] and Kishimoto[8] explain that electrons hopping between Fe^{2+} and Fe^{3+} ions may reduce the activation energy of Co^{2+}-ion migration. From another point of view, the hopping of electrons may help to maintain the local neutrality, thus facilitating the migration of Co^{2+} ions.

The thermal stability of the coercivity of $(Co\text{-}Fe_3O_4)_{1-x}$ $(Co\text{-}\gamma\text{-}Fe_2O_3)_x$ particles with various Fe^{2+}-ion contents is shown in Fig. 15. The thermal stability of the coercivity increases with the oxidation degree x of the particles. For completely oxidized particles (i.e., Co-γ-Fe_2O_3 particles), the oxidation degree is $x = 1$. According to Fig. 15, the coercivities of pure $Co\text{-}Fe_3O_4$ and Co-γ-Fe_2O_3 particles at 100 °C are about 65% and 75% of those at room temperature, respectively. The coercivity of $(Co\text{-}Fe_3O_4)_{1-x}(Co\text{-}\gamma\text{-}Fe_2O_3)_x$ particles with $(Fe^{2+}/\text{total Fe})$ molar ratio of 0.2 at 100 °C is about 70% of that at room temperature. The coercivities of these particles are all higher than that of CrO_2 particles (see Fig. 14). And the high-temperature stabilities of the coercivity of these particles are all better than that of CrO particles.[4] Although the coercivity of Co-γ-Fe_2O_3 particles is lower than that of $Co\text{-}Fe_3O_4$ particles with the same cobalt content, the thermal stability is better.

The coercivity of $Co\text{-}Fe_3O_4$ particles is changed with time even at room temperature. We find that this aging effect is dependent on the cooling rate after reduction (Co-α-$Fe_2O_3 \rightarrow Co\text{-}Fe_3O_4$). Lower cooling rate will get higher coercivity and less aging effect, as shown in Figs. 16 and 17. The cobalt content of the particles of Figs. 16 and 17 is (Co/Co + Fe) = 6 mol %. From Fig. 16 we can see that the coercivity of $Co\text{-}Fe_3O_4$ particles is increased as cooling rate decreased. The increasing of coercivity is remarkable for

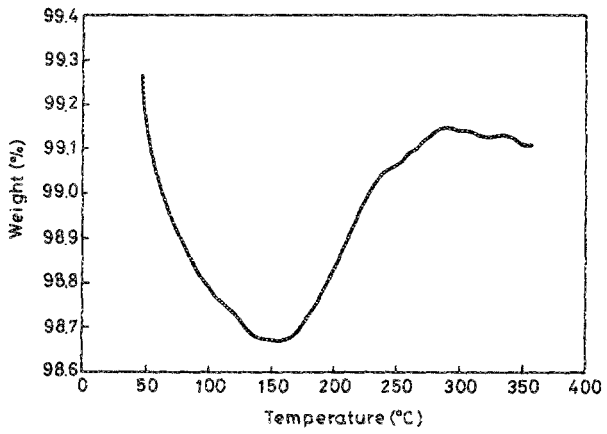

FIG. 10. TGA analysis of the $Co\text{-}Fe_3O_4$ particles (Co/Co + Fe = 6 mol %).

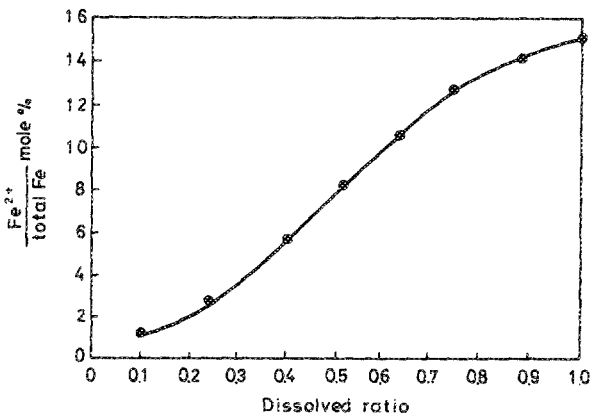

FIG. 12. Variation of Fe^{2+} content with the dissolved ratio of partially oxidized $Co\text{-}Fe_3O_4$ particles (Co/Co + Fe = 6 mol %).

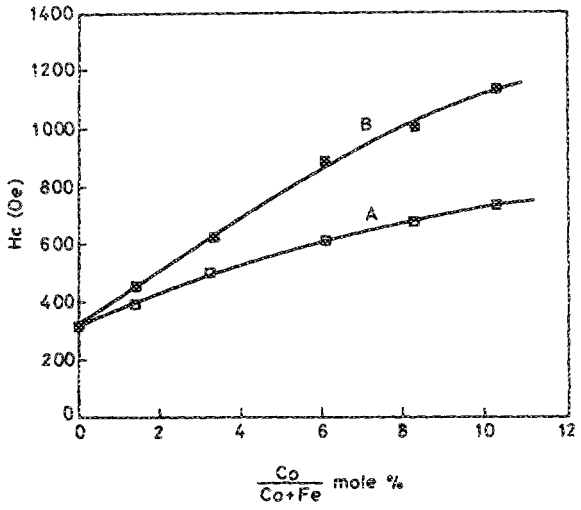

FIG. 13. Dependencies of coercivity on the cobalt content of Co-γ-Fe_2O_3 particles (curve A) and Co-γ-Fe_2O_3 particles (curve B) after being annealed in N_2 at 350 °C for 3 h.

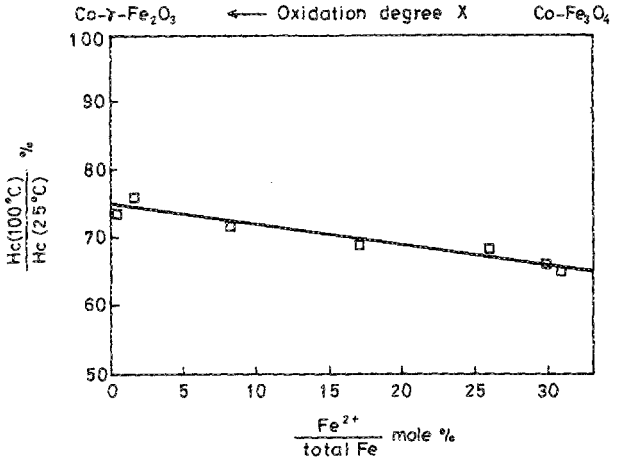

FIG. 15. Relationship between the thermal stability of the coercivity of the $(Co\text{-}Fe_3O_4)_{1-x}$ $(Co\text{-}\gamma\text{-}Fe_2O_3)_x$, particles and their degree of oxidation. Cobalt content of the particles is (Co/Co + Fe) = 6 mol %.

slowly cooled particles. Since a lower cooling rate will cause Co^{2+} ions to diffuse deeper into the particles, coercivity of the particles will be higher. Coercivity of the very slowly cooled particles can reach about 1000 Oe. Figure 17 shows the variation of coercivity with aging time. The cooling rates of the Co-Fe_3O_4 particles of curves S_1, S_2, and S_3 are 65, 10, and 1.5 °C/min, respectively. However, the coercivity of Co-γ-Fe_2O_3 particles does not have this aging effect, as shown in curve S_0. As the Co-Fe_3O_4 particles are aged at room temperature, the coercivity is increased at the initial stage of aging and saturated when the aging time is longer than 80 days. For rapidly quenched Co-Fe_3O_4 particles, the increase of coercivity with aging time is evident. By the dissolution method we find that the distributions of Co^{2+} ions within Co-Fe_3O_4 particles are about the same for just-quenched particles and the particles after 80 days aged in room temperature. The reason is that the unstable Co^{2+} ions in the crystal lattices of quenched particle will move to more stable lattice sites gradually (due to the presence of Fe^{2+}) at room temperature. This can be explained by the following experiment.

If the Co-Fe_3O_4 particles (cooling rate = 10 °C/min) are aged at room temperature for 85 days (H_c is about saturated) then heated to 100 °C in N_2 and quenched, the coercivity will drop abruptly then increase gradually with time, as shown in Fig. 18. This may be due to the fact that many Co^{2+} ions will migrate to neighboring unstable sites (in the same region of the particle) if the particles are heated with short time that is not enough to cause Co^{2+} ions diffusing deeper into the particles. Owing to the random occupation of unstable Co^{2+} ions, the coercivity of the Co-Fe_3O_4 particles which just quenched from 100 °C is lowered (see Fig. 15). At room temperature, these unstable Co^{2+} ions will migrate to the more stable lattice sites gradually by the spontaneous magnetic field along the long axis of the acicular particles,[8] and so the coercivity increases with time again. On the other

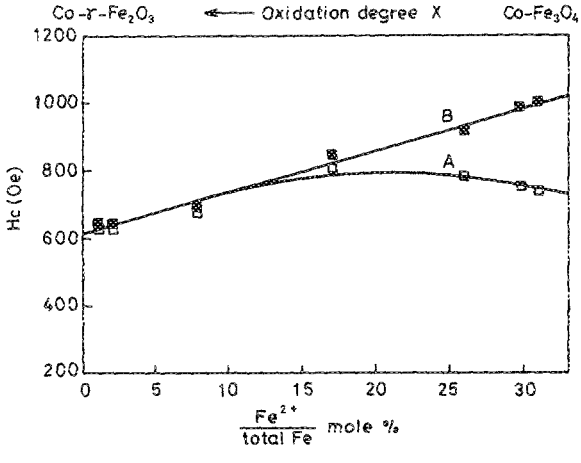

FIG. 14. Relationships between the coercivity and Fe^{2+} content of the $(CoFe_3O_4)_{1-x}$ $(Co\text{-}\gamma\text{-}Fe_2O_3)_x$ particles (Co/Co + Fe = 6 mol %). Curve B is the coercivities of the particles of curve A after they were aged at room temperature for 80 days.

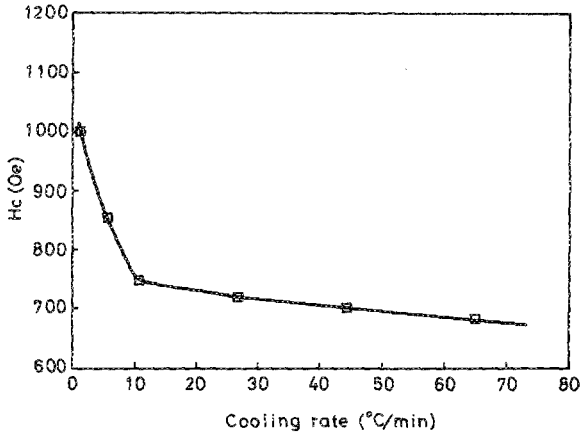

FIG. 16. Dependence on cooling rate of the coercivity of the Co-Fe_3O_4 particles (Co/Co + Fe = 6 mol %).

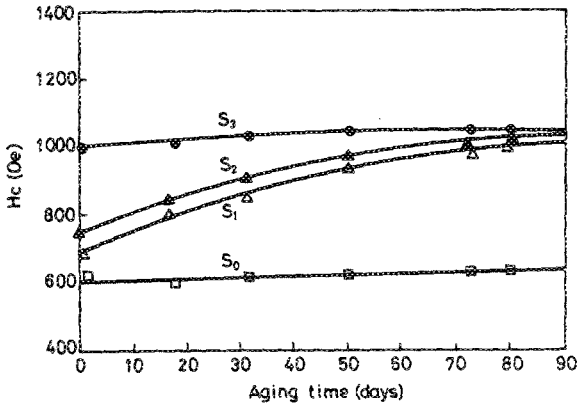

FIG. 17. Variations of coercivities with time at room temperature. Curves S_1, S_2, and S_3 are coercivities of the Co-Fe_3O_4 particles with cooling rates of 65, 10, and 1.5 °C/min, respectively. Curve S_0 is coercivities of the Co-γ-Fe_2O_3 particles. Cobalt content of the particles is $(Co/Co + Fe) = 6$ mol %.

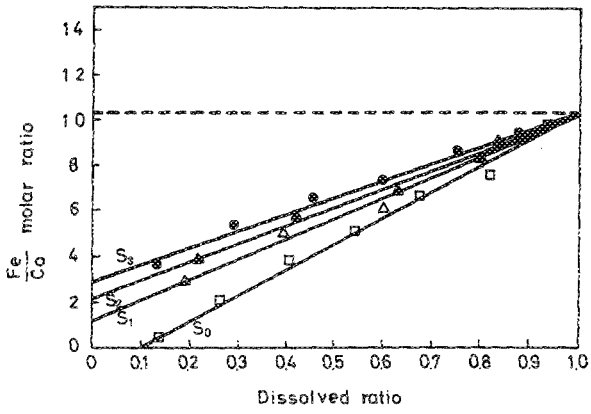

FIG. 19. Variation of Fe/Co molar ratio with dissolved ratio for three kinds of particles. Curve S_0 is the Co-α-FeOOH particles. Curve S_1 and S_2 are the Co-Fe_3O_4 particles with cooling rates of 10 and 1.5 °C/min after reduction, respectively. Curve S_3 is the Co-γ-Fe_2O_3 particles.

hand, Sawatzky, van der Woude, and Morrish[12] had shown that the amount of Co^{2+} ions at tetrahedral-*A* sites for quenched $CoFe_2O_4$ particles was larger than that of slowly cooled particles. In $CoFe_2O_4$ crystal, the stable site for the Co^{2+} ion is octahedral-*B* site.

Although the number of unstable Co^{2+} ions within quenched Co-Fe_3O_4 particles is larger than that of slowly cooled particles, the saturation coercivity of quenched particles is still lower than that of slowly cooled particles (see Fig. 17), because slowly cooled particles have deeper Co^{2+}-ion distribution. The $(Co\text{-}Fe_3O_4)_{1-x}(Co\text{-}\gamma\text{-}Fe_2O_3)_x$ particles with small x also have evident cooling-rate-dependent aging effect.

The distribution of Co^{2+} ions within our particles is measured by the dissolution method. Figure 19 shows the relations between Fe/Co molar ratio and dissolved ratio of various particles. The particles are completely dissolved when the dissolved ratio is equal to 1.0. For the dissolved ratio of 0.5 means that the outer half part of the particle is dissolved. From Fig. 19 we can see that the cobalt content (Co/Fe) of the particles is about 10 mol %, and the amount of cobalt is decreased from particle surface to the inner part. Curve S_0 is the Co-α-FeOOH particles. Curves S_1 and S_2 are the Co-Fe_3O_4 particles with cooling rates of 10 and 1.5 °C/min after reduction, respectively. Curve S_3 is the Co-γ-Fe_2O_3 particles which were oxidized from sample S_2. The nonuniformity of Co-ion distribution is proportional to the slope of the curve. Larger slope of the curve means that more Co^{2+} ions localized in the outer layer of the particle. The horizontal dotted line indicates that the Co^{2+} ions within the particles are homogeneously distributed. From Fig. 19 we can see that Co^{2+} ions will diffuse more deeply into the Co-Fe_3O_4 particles, if the particles are cooled slowly after reduction.

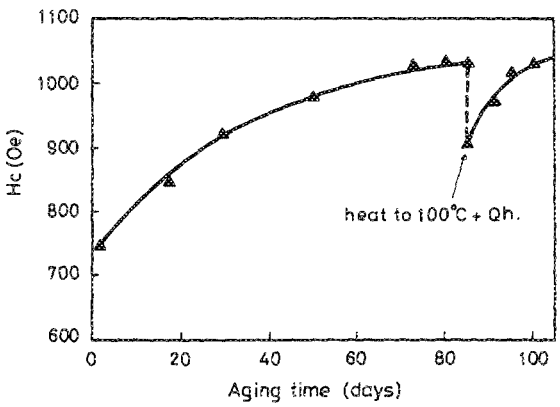

FIG. 18. Variation of the coercivity of the Co-Fe_3O_4 particles with time at room temperature.

IV. CONCLUSIONS

In the $FeCl_2$-NaOH reaction system, acicular α-FeOOH particles can be formed if the molar ratio of NaOH/$FeCl_2$ in the mixed solution is larger than 2. Higher concentration of the solution or higher reaction temperature will result in larger precipitated particles.

In the coating of cobalt on α-FeOOH particles, the adding of $CoSO_4$ solution shall be very slow. Otherwise, new particles will be precipitated and fail the coating. In the dehydration process, N_2 is a better atmosphere than air or H_2.

Distributions of Co^{2+} and Fe^{2+} ions within the Co-modified iron oxide particles can be determined by the "dissolution method." For acicular Co-modified iron oxide particles, higher Fe^{2+}-ion content will have higher saturation magnetization; higher cobalt content will have higher coercivity. However, increasing Fe^{2+}-ion content will decrease thermal stability of the coercivity. Co^{2+}-ion distribution and coercivity of the Co-Fe_3O_4 particles are dependent on the cooling rate after reduction. Slowly cooled Co-Fe_3O_4 particles will have deeper Co^{2+}-ion distribution and higher coercivity than those of rapidly cooled Co-Fe_3O_4 particles.

As Co-Fe_3O_4 particles are aged at room temperature, the increase of the coercivity with time is due to the migra-

tion of unstable Co^{2+} ions to the more stable lattice sites by the spontaneous magnetic field along the long axis of the acicular particles. If the Co-γ-Fe_2O_3 particles are annealed in N_2 at 350 °C, coercivity of the particles will be increased due to the diffusion of Co^{2+} ions into the particles. The increment of the coercivity is approximately proportional to the cobalt content of the particles.

ACKNOWLEDGMENT

The authors wish to acknowledge the National Science Council of Taiwan, R.O.C. for the financial support of this work under Grant No. NSC78-0405-E002-09.

[1]L. R. Bickford, Jr., J. Pappis, and J. L. Stull, Phys. Rev. **99**, 1210 (1955).
[2]L. R. Bickford, Jr., J. M. Brownlow, and R. F. Penoyer, Proc. Inst. Electr. Eng. Part B **104**, Suppl. No. 5, 238 (1957).
[3]S. Umeki, S. Saitoh, and Y. Imaoka, IEEE Trans. Magn. **MAG-10**, 655 (1974).
[4]Y. Imaoka, S. Umeki, Y. Kubota, and Y. Tokuoka, IEEE Trans. Magn. **MAG-14**, 649 (1978).
[5]M. Kishimoto, T. Sueyoshi, J. Hirata, M. Amemiya, and F. Hayama, J. Appl. Phys. **50**, 450 (1979).
[6]M. Amemiya, M. Kishimoto, and F. Hayama, IEEE Trans. Magn. **MAG-16**, 17 (1980).
[7]M. Kishimoto, S. Kitaoka, H. Andoh, M. Amemiya, and F. Hayama, IEEE Trans. Magn. **MAG-16**, 3029 (1981).
[8]M. Kishimoto, IEEE Trans. Magn. **MAG-15**, 906 (1979).
[9]G. Bate, in *Ferromagnetic Materials*, edited by E.P. Wohlfarth (North-Holland, Amsterdam, 1980), Vol. 2, p.417.
[10]H. Kojima and K. Hanada, IEEE Trans. Magn. **MAG-16**, 11 (1980).
[11]A. Yanase, J. Phys. Soc. Jpn. **17**, 1005 (1962).
[12]G.A. Sawatzky, F. van der Woude, and A. H. Morrish, J. Appl. Phys. **39**, 1204 (1968).